

A Model of the Muon

R. WAYTE

29 Audley Way, Ascot, Berkshire SL5 8EE, England, UK

email: rwayte@googlemail.com

Abstract. A geometrical/mechanical model of the muon has been developed based on a previous detailed model of the electron and the fine structure constant. The anomalous magnetic moment and lifetime have been calculated in terms of muon component parts. Known features of the tauon have also been related to the muon.

PACS: 14.60.Ff

Submitted to Journal of Physics G: Nuclear and Particle Physics.

1. Introduction

Muons behave very much like heavy electrons, with identical charge and spin, plus fairly similar anomalous magnetic moment. However, two different features are apparent: the lifetime of $2.2 \mu\text{sec}$, and a possible mass defect. Analysis of muon structure is therefore expected to follow the electron analysis in essence (Wayte, Paper 1) but some additional aspects should appear. Since it is impossible to dissect a muon, all proposed design has to be arbitrary, but total consistency with experiment is achievable. All physical constants and

muon parameters have been taken from <http://physics.nist.gov/constants> and <http://pdg.lbl.gov> .

As for the electron model, the classical laws of energy and momentum hold continuously in 4-dimensional spacetime, and the muon as a whole must behave in accordance with relativity theory. Features peculiar to the muon will be described in some detail, while features already covered by the electron model will be briefly outlined only. Some basic properties of the muon model will now be mentioned before entering the full analysis. Overall, the muon has the appearance of a helically wound hollow torus, wherein the winding material is itself a thinner continuous helix, see figure 1. For visualisation purposes, the individual helical turns are referred to as 'particles' throughout the analysis of muon structure. Muon mass is the matter/energy which constitutes and runs through this structure at the velocity of light.

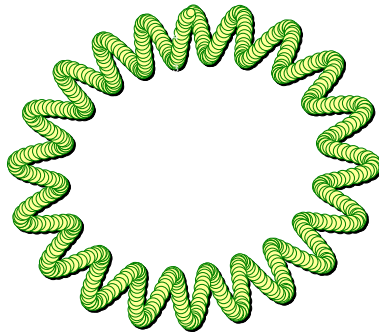


Figure 1. General illustration of toroidal muon, with its helix-upon-helix structure. (Not to scale).

Muon spin results may be interpreted to suggest that the spin radius is ($r_{\mu} = 137 r_{\mu 0}$), where ($r_{\mu 0} = e^2 / m_{\mu} c^2$) is the theoretical classical radius. Half the muon energy is in its exterior non-rotating electromagnetic field, and half is core material spinning at velocity c . So angular momentum of the muon is given by:

$$s_{\mu} = (m_{\mu} / 2) c r_{\mu} = \hbar / 2 \quad . \quad (1.1)$$

In order to maintain the charged helical material 'particles' in this rapidly spinning torus, a guidewave quantum field of material is predicted to exist around the loop, capable of confining them. This field interacts with any applied magnetic field and accounts for the

anomalous magnetic moment. The charged particles spin around the muon toroidal periphery at the velocity of light, in period ($\tau_\mu = 2\pi r_\mu/c$) so the periphery is equal to the Compton wavelength ($\lambda_{C\mu} = h/m_\mu c$), and the muon's electromagnetic field will be modulated at Compton frequency ($\nu_{C\mu} = c/\lambda_{C\mu}$).

The muon has running helix-upon-helix substructures around the main torus of spin radius r_μ . The periphery of this spin-loop contains 137 smaller toroidal core-segment 'particles' of radius $(\pi/2)r_{\mu 0}$, which may be clumped into 3 separate but linked packs. Each of these core-segments consists of 37 smaller pearl 'particles' around its periphery. These similarly have 137 smaller grain 'particles' around their peripheries, and each of these has 24 smaller mite 'particles' around it. Then each mite has 50 fundamental elements around it, which are the real source of electromagnetic field quanta. Thus the muon charge consists of a complex assembly of $(137 \times 37 \times 137 \times 24 \times 50)$ elemental charges.

Each particle species will be shown to grow from a smaller seed-particle into its final size, starting with the largest species (r_μ) in order to make room for the next smaller species, and so-on downwards. Apparently, the seeds are *created* in turn *as required*, rather than existing in some pre-muon structure. This eliminates the problem of "lesser-fleas upon little fleas, ad-infinitum".

Muon mass will be neatly expressed in terms of the electron mass, and a feasible explanation for its absolute value has been discovered. The mass is due entirely to the local material circulating at the velocity of light, plus an attached external electromagnetic field. No Higgs mechanism is necessary.

2. Muon anomalous magnetic moment

For the basic muon model, the spin-loop would be expected to produce a classical magnetic moment:

$$\mu_s = \text{current} \times \text{area} = \left(\frac{ec}{2\pi r_\mu} \right) (\pi r_\mu^2) = \frac{e\hbar}{2m_\mu} . \quad (2.1)$$

The measured value is slightly higher than this because of the anomalous component:

$$\mu_\mu = \mu_s \times 1.001\,165\,92069(60) . \quad (2.2)$$

Comparison of this with the electron magnetic moment in Paper 1 reveals that the muon possesses a different internal mechanism, but there are some features in common. Our muon model produces a concise expression for μ_μ as:

$$\mu_\mu / \mu_s = 1.001165920696 = \{1 + \alpha / 2\pi\} \left\{ 1 + \alpha^2 \pi \delta [1 + 2\alpha(1 + (4/\pi)\varepsilon[1 - (\pi/e_n)\mu])]\right\}. \quad (2.3)$$

Here the fine structure constant has been taken as the current empirical value:

$$\alpha^{-1} = 137.035\,999\,679(94) \quad , \quad (2.4)$$

while the pearl structure constant is ($\delta = 1/12\pi \sim 1/37.7$), the grain structure constant is ($\varepsilon = 1/24$), the mite structure constant is ($\mu = 1/16\pi \sim 1/50$), and $e_n = 2.71828$ is the natural logarithm base.

The most significant part of Eq.(2.3) is the first curly bracket which represents muon total electric field energy, including that in the spin-loop guidewave. As for the electron, the total energy of the muon's external electric field is $(1/2)m_\mu c^2$, so that the remaining $(1/2)m_\mu c^2$ of the muon's energy must reside in the core-segments and spin-loop guidewave. The electric self-interaction energy of the muon due to the spin-loop is $e^2/2\pi r_\mu$, as calculated by the method of Paper 1. In contrast to the electron, however, this energy appears to come directly from the creation source rather than the muon's own energy. Consequently, the muon magnetic moment should approach:

$$\mu \approx (e\hbar/2m_\mu)[1 + (e^2/2\pi r_\mu) / m_\mu c^2] = (e\hbar/2m_\mu)(1 + \alpha/2\pi). \quad (2.5)$$

The second curly bracket of Eq.(2.3) contains correction terms due to the finite areas of pearls, grains, mites, and elements which produce their own magnetic moments. According to the positive signs, these are effectively parallel to the spin-loop except for the elements, in contrast to the negative sign for the electron pearls, etc. Core-segments travel around the spin-loop circumference at velocity c but are oriented orthogonally to the circumference, so do not contribute to the muon magnetic moment, see figure 2.1. As illustrated, flow of material through a particle centre against the direction of particle propagation is the high energy state. Evidently, if a muon has overall negative helicity, then the core-segments must have negative helicity (a higher energy state), but the pearls then have positive helicity (a higher energy state). Likewise, the grains occupy higher energy by

flipping back to negative helicity; and the mites flip back to positive helicity, which is a higher energy state. The final elements take the low energy state.

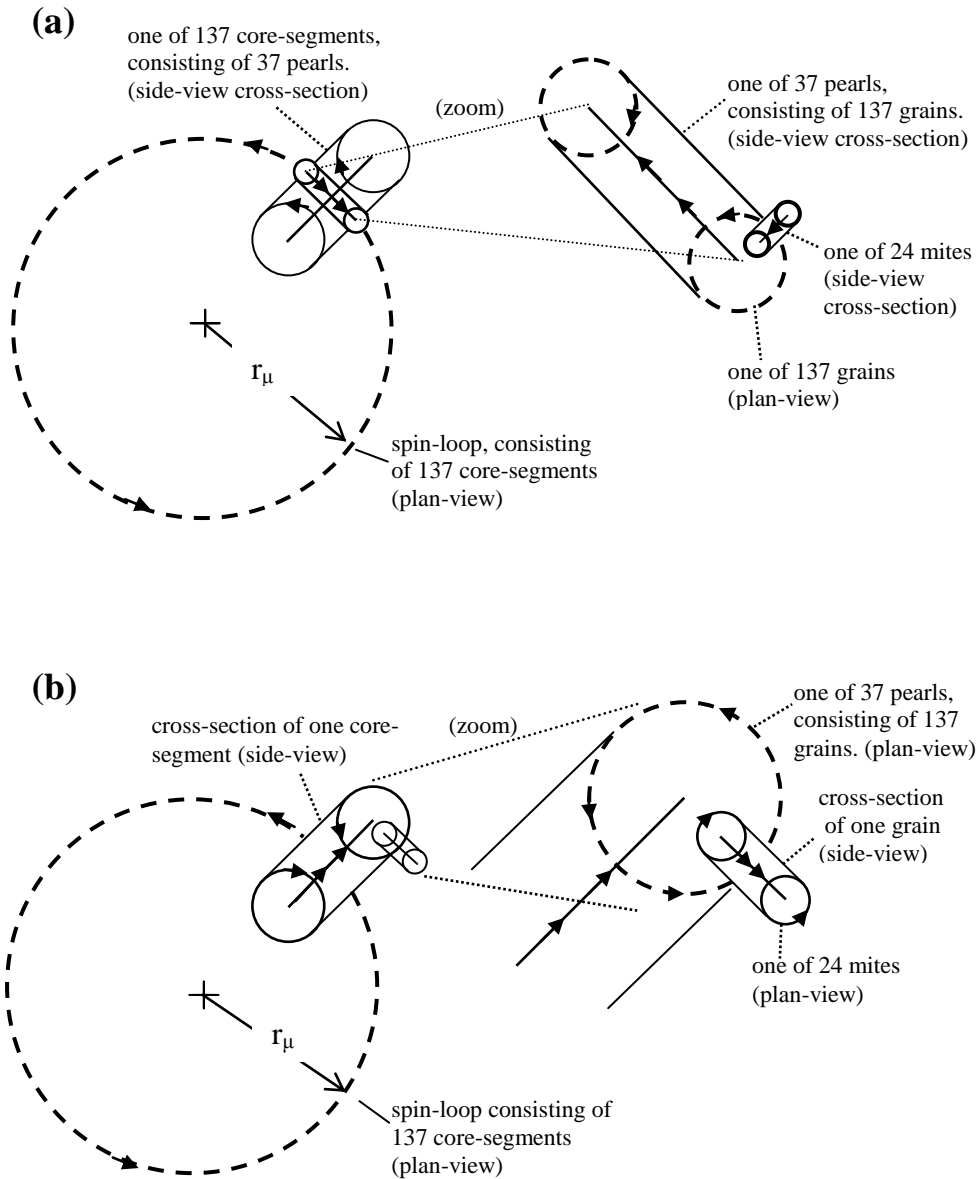


Figure 2.1a,b Schematic diagram of a cross-sectional view of the muon spin-loop, showing one core-segment with one pearl containing one grain and one mite. Drawn not-to-scale, to illustrate the orthogonal structure of the assembly, with suggested directions of travel for all particles.

Contribution of magnetic moment by the pearls, grains, mites, and elements, must again be due to the helicity since these particles continually change direction in 3 dimensions during their travels. Physical meaning may be attributed to each part of the second bracket in Eq.(2.3) by reduction as follows:

$$\left\{ 1 + \left(\frac{1}{137} \right) \left[\frac{2 \times (137 \times 37.7)}{(137(2/\pi) \times 37.7)^2} \left(\frac{2}{\pi} \right) \right] \left[1 + 2 \left(\frac{2}{\pi} \right) \frac{137}{(137(2/\pi))^2} \left(\frac{2}{\pi} \right) \left(1 + 2 \left(\frac{\pi}{2} \right) \frac{24}{(24(\pi/2))^2} \left[1 - \left(\frac{\pi}{e_n} \right) \frac{50}{50^2} \right] \right) \right] \right\} .$$

(137 x 37 pearls) (137 grains) (24 mites) (50 elements) (2.6)

For clarity, the short forms of α , δ , ϵ , and μ have been used here.

Factor (1/137) at the beginning represents the interaction coefficient between the above helical particle orbits and the external magnetic field, this being 137 times weaker than that for the main spin-loop magnetic moment.

The following square bracket describes the magnetic moment of 37 pearls in each of 137 core-segments around the spin-loop. Each pearl has area $(137(2/\pi) \times 37.7)^2$ times less than the spin-loop area. Coefficient 2 implies that the pearl magnetic moment is doubled because of the enhanced second harmonic guidewave action, as for the electron grains in Eq.(2.5.12) of Paper 1. Factor $(2/\pi)$ is necessary because the projected areas of the circulating pearls *parallel* to the spin-loop are reduced to $(2/\pi)$ on average.

The second square bracket contains analogous terms for grains. Factor $137/(137(2/\pi))^2$ covers 137 grains per pearl, each of area $(137(2/\pi))^2$ times less than a pearl area. Coefficient 2 is for weighting, as in Eq.(3.3.2). Factor $(2/\pi)$ is due to the helicity of these grains being $(2/\pi)$ rather than unity. Attenuation coefficient $(2/\pi)$ is due to the second degree of movement the grains areas have, relative to the spin-loop orientation.

The next round bracket accounts for 24 mites per grain, each of area $(24(\pi/2))^2$ times less than a grain area. Coefficient 2 is for weighting. Factor $(\pi/2)$ is there for the mite propagation velocity around the grain being c' , while their spin velocity is only c . The two previous projected area factors $(2/\pi)$ are still required by these mites

In the last square bracket, factor $50/50^2$ covers 50 effective number of elements per mite, each of area 50^2 times less than a mite area. Factor (π/e_n) is for weighting to include internal field energy, as in Eq.(3.5.4).

Finally, it is interesting to compare Eq.(2.3) with the equivalent QED magnetic moment anomaly:

$$a(\text{QED}) \approx 0.5 \left(\frac{\alpha}{\pi} \right) + 0.765857410 \left(\frac{\alpha}{\pi} \right)^2 + 24.05050964 \left(\frac{\alpha}{\pi} \right)^3 + \dots \quad (2.7)$$

If Eq.(2.3) is expanded as a series in (α/π) , while letting $(\delta = 1/12\pi)$, we get:

$$a(\text{Eq.}(2.3)) \approx \frac{1}{2} \left(\frac{\alpha}{\pi} \right) + \frac{\pi^2}{12} \left(\frac{\alpha}{\pi} \right)^2 + \left(\frac{\pi^2}{24} + \frac{4\pi^3}{24} \right) \left(\frac{\alpha}{\pi} \right)^3 + \dots \quad (2.8)$$

These square and cubic terms differ from Eq.(2.7), so QED is not compatible with this real model.

3. Detailed muon structure

Since a muon is essentially a heavy electron, its design is to be based upon the fine structure constant $(\alpha = e^2/\hbar c \approx 1/137.036)$. This secures agreement with experiment regarding spin, charge and general magnetic moment. However, analysis of the anomalous magnetic moment in the previous Section revealed that the inner-structure of the muon differs from that of the electron. Calculation of a mass-defect for the muon will also agree with the proposed internal design.

3.1 Creation of a muon spin-loop

Muon spin-loop design is more similar to an electron's core-segment than its spin-loop. Section (2.1) of Paper 1 contains all the necessary derivation for the muon spin-loop spiralling process, but the nomenclature has to be changed. The muon spiralling action-integral is then based upon the expression:

$$\ln 137 - \ln[1 + \ln 137] \approx \pi \quad , \quad (3.1.1a)$$

which may be reduced to:

$$\int_{O_{\mu s}}^{O_{\mu}} \frac{e^2}{z} \left(1 - \frac{v_z}{c} \right) \left[\frac{v_z}{c} \right] dt \approx \int_0^{2\pi} \left(\frac{m_{\mu}}{2} \right) cr_{\mu o} d\theta \approx 3 \times \int_0^{2\pi/3} \left(\frac{m_{\mu}}{2} \right) cr_{\mu o} d\theta \quad , \quad (3.1.1b)$$

where $(e^2/c = m_{\mu} cr_{\mu o})$ and $O_{\mu s}$ is the initial spin-loop-seed circumference, which grows by 137 times to the final spin-loop circumference $O_{\mu} = 2\pi r_{\mu} = 137 O_{\mu s}$. The final integral

allows for the possible agglomeration of core-segments into 3 separate packs after spiralling, as implied later in the mass analysis. Acceleration of the 137 core-segments in the spin-loop up to velocity c could be described by adapting Section (2.2) of Paper 1.

The action-integral describing the *final equilibrium* spin-loop circumference of 137 core-segments is derived from:

$$\ln 137 \approx \pi^2 / 2 \quad , \quad (3.1.2a)$$

which reduces to:

$$\int_{y_o=2\pi r'_o}^{137 y_o} \frac{e^2}{y} dt \approx \int_0^{2\pi} \frac{m_\mu}{2} cr_{\mu o} d\theta \approx 3 \times \int_0^{2\pi/3} \frac{m_\mu}{2} cr_{\mu o} d\theta \quad , \quad (3.1.2b)$$

where $r'_o = r_{\mu o} (\pi/2)$ is the core-segment radius, and $dt = dy/c(\pi/2)$ signifies that they rotate at velocity $c' = c(\pi/2)$. Clearly, these muon core-segments are designed like electron-pearls, thus far. They propagate at the velocity of light around the muon spin-loop, producing spin ($1/2$) and a magnetic moment.

3.2 Creation of a muon core-segment

Muon core-segment structure is like that of an electron's pearl design, in that there are 37 pearls spinning and travelling around the core-segment circumference. Section (2.5) of Paper 1 contains the necessary derivation for spiralling and acceleration processes, plus the final pearly charge helix propagating at velocity c' around each core-segment. In terms of muon nomenclature, the creation spiralling action-integral is derived from:

$$\ln\left(\frac{37.7}{e_n}\right) - \ln\left[1 + \ln\left(\frac{37.7}{e_n}\right)\right] + \ln 37.7 \approx \frac{\pi^2}{2} \quad , \quad (3.2.1a)$$

Then upon introducing ($e^2/c = m_\mu cr_{\mu o}$), this reduces to:

$$\int_{'O_{os}}^{'O_o} \frac{(e/137)^2}{z} \left\{1 - \frac{v_z}{c'}\right\} \left[\frac{v_z}{c'}\right] dt + \int_{'O_{1s}}^{37.7'O_{1s}} \frac{(e/137)^2}{z_h} dt \approx \int_0^{2\pi} \frac{m_\mu cr_{\mu o}}{2 \times 137^2} d\theta \quad , \quad (3.2.1b)$$

where $'O_{os}$ is the original core-segment-seed circumference, and the core-segment final circumference is ($'O_o = 2\pi r'_o = 'O_{os}(37.7/e_n)$), and $dt = dz/c'$. In the second term, the

original core-segment-seed circumference has 37.7 material turns (pearl-seeds 'O_{1s}) in a helix created just prior to the spiralling. These grow in the muon final core-segment into 37.7 pearls (each of circumference 'O₁ = 'O₀ /37.7), which propagate along the circumference at velocity c' and spin orthogonally at velocity c'

The action-integral describing the final core-segment's circumferential helix of 37.7 pearls spinning at velocity c' is derived from:

$$\ln 37.7 \approx \pi^2 / e_n \quad , \quad (3.2.2a)$$

which may be reduced to:

$$\int_{'O_1}^{37.7'O_1} \frac{(e/137)^2}{y} \cdot \frac{dy}{c'} \approx 2 \int_0^{2\pi} \frac{m_\mu c r_{\mu 0}}{2 \times 137^2} \left(\frac{1}{e_n} \right) d\theta \quad , \quad (3.2.2b)$$

where 'O₁ = 'O₀ /37.7 is a pearl circumference.

3.3 Creation of a muon pearl

Muon pearl design incorporates 137 grains travelling around the pearl at velocity c' while spinning at velocity c'. Its creation spiralling stage and original seed structure can be based on the formula;

$$\ln \left(\frac{137}{e_n} \right) - \ln \left[1 + \ln \left(\frac{137}{e_n} \right) \right] + \ln 137 \approx \left(\frac{2\pi^2}{e_n} \right) \quad . \quad (3.3.1)$$

This may be developed in the usual way to produce a pearl creation spiral action-integral:

$$\int_{'O_{1s}}^{'O_1} \frac{(e/137 \times 37.7)^2}{\ell} \left\{ 1 - \frac{v_\ell}{c'} \right\} \left[\frac{v_\ell}{c'} \right] dt + \int_{'O_{2s}}^{137'O_{2s}} \frac{(e/137 \times 37.7)^2}{\ell_h} dt \approx \int_0^{2\pi} \frac{m_\mu c r_{\mu 0}}{(137 \times 37.7)^2} \left(\frac{2}{e_n} \right) d\theta \quad , \quad (3.3.2)$$

where 'O_{1s} is the pearl-seed circumference, which grows to the final pearl circumference 'O₁ = 'O_{1s} (137/e_n). In the second term, the original pearl-seed circumference has 137 material turns (grain-seeds 'O_{2s}) in its circumferential helix created just prior to spiralling. These grow in the final pearl into 137 grains, so a muon pearl circumference consists of 137

grains (each of circumference $'O_2 = 'O_1/137$), which propagate along the circumference at velocity c' and spin orthogonally at velocity c , according to the formula:

$$\ln 137 \approx \pi^2 / 2, \quad (3.3.3)$$

which may be reduced to:

$$\int_{'O_2}^{137'O_2} \frac{(e/137 \times 37.7)^2}{\xi} \frac{d\xi}{c'} \approx \int_0^{2\pi} \frac{m_\mu c r_{\mu o}}{2(137 \times 37.7)^2} d\theta \quad . \quad (3.3.4)$$

3.4 Creation of a muon grain

Muon grain design incorporates 24 mites travelling around the grain at velocity c' while spinning at velocity c . Its creation spiralling stage and original seed structure can be based on the formula;

$$[\ln 24 - \ln(1 + \ln 24)] + \ln 24 \approx \pi^2 / 2. \quad (3.4.1)$$

Thus, each grain-seed grows by spiralling from its seed state according to this action-integral:

$$\int_{'O_{2s}}^{'O_2} \frac{(e/137 \times 37.7 \times 137)^2}{\xi} \left\{ 1 - \frac{v_\xi}{c'} \right\} \left[\frac{v_\xi}{c'} \right] dt + \int_{'O_{3s}}^{24'O_{3s}} \frac{(e/137 \times 37.7 \times 137)^2}{\xi_h} dt, \quad (3.4.2)$$

$$\approx \int_0^{2\pi} \frac{m_\mu c r_{\mu o}}{2(137 \times 37.7 \times 137)^2} d\theta$$

where the grain-seed circumference is $'O_{2s}$, and its final grain circumference is ($'O_2 = 'O_{2s} \times 24$). In the second term, the original grain-seed circumference has 24 material turns (mite-seeds $'O_{3s}$) in a helix created just prior to spiralling. These grow in the final grain into 24 mites, so a muon grain circumference $'O_2$ consists of 24 mites, which propagate along the circumference at velocity c' but spin orthogonally at velocity c , according to the formula:

$$\ln 24 \approx \pi, \quad (3.4.3)$$

which reduces to:

$$\int_{'O_3}^{24'O_3} \frac{(e/137 \times 37.7 \times 137)^2}{\xi} \frac{d\xi}{c} \approx \int_0^{2\pi} \frac{m_\mu c r_{\mu o}}{2(137 \times 37.7 \times 137)^2} d\theta \quad . \quad (3.3.4)$$

3.5 Creation of a muon mite

Muon mite design incorporates 50 elements travelling around the mite at velocity c while spinning at velocity c . Its spiralling stage and original seed structure can be based on the formula;

$$[\ln 50 - \ln(1 + \ln 50)] + \ln 50 \approx 2\pi. \quad (3.5.1)$$

Thus, each mite-seed grows by spiralling from its seed state according to this action-integral:

$$\int_{'O_{3s}}^{'O_3} \frac{(e/137 \times 37.7 \times 137 \times 24)^2}{\xi} \left\{ 1 - \frac{v_\xi}{c} \right\} \left[\frac{v_\xi}{c} \right] dt + \int_{'O_{4s}}^{50'O_4s} \frac{(e/137 \times 37.7 \times 137 \times 24)^2}{\xi_h} dt, \quad (3.5.2)$$

$$\approx \int_0^{2\pi} \frac{m_\mu c r_{\mu o}}{(137 \times 37.7 \times 137 \times 24)^2} d\theta$$

where the seed circumference is $'O_{3s}$, and its final circumference is ($'O_3 = 'O_{3s} \times 50$). In the second term, the original mite-seed circumference has 50 material turns (element-seeds $'O_{4s}$) in a helix created just prior to spiralling. These grow in the final mite into 50 elements, so a muon mite circumference consists of 50 elements (each of circumference ($'O_4 = 'O_3 / 50$)), which propagate along the mite circumference at velocity c and spin orthogonally at velocity c , according to the formula:

$$\ln 50 \approx \pi(\pi/e_n), \quad (3.5.3)$$

which reduces to:

$$\int_{'O_4}^{50'O_4} \frac{(e/137 \times 37.7 \times 137 \times 24)^2}{\sigma} \frac{d\sigma}{c} \approx \left(\frac{\pi}{e_n} \right) \times \int_0^{2\pi} \frac{m_\mu c r_{\mu o}}{2(137 \times 37.7 \times 137 \times 24)^2} d\theta. \quad (3.5.4)$$

Factor (π/e_n) on the right side accounts for the internal field energy associated with the element's material energy. Motion of elements around their mites and higher species produces field modulation, which is most coherent at the Compton frequency because of the fixed muon spin axis.

3.6 Muon charge uniqueness

Previous calculations of creation action depended upon the charge being divisible among the various sub-structures; so we need a formula to describe the fundamental charge of the elements in a muon. One was found for the electron which was based upon allocating 3 fragments of charge Δq to each element. These were visualized as 3 localized material curls constituting the element circumference, plus some field material holding the 3 charge-curls in place, effectively increasing their weight to $3(\pi/e_n)$. Now the total number of elements per muon is given by Eq.(2.6) as:

$$n_\mu = 137 \times 37.7 \times 137 \times 24 \times 50 = 8.5405 \times 10^8 \quad . \quad (3.6.1)$$

This is the same as for the electron, so muon charge is equally unique:

$$e = n_\mu \times 3(\pi/e_n) \times \Delta q = 2.961135 \times 10^9 \Delta q \quad . \quad (3.6.2)$$

4. Muon mass

Absolute mass of the muon is unexplained but there are some design features which relate it to electronic mass, ($m_e = 9.109\,382\,15(45) \times 10^{-31}$ kg). For example, the latest empirical value is:

$$m_\mu/m_e = 206.768\,2823(52) \quad , \quad (4.1)$$

which is slightly less than $3 \times 69 = 207$. Factor 69 could indicate that the spin-loop actually consists of 3 distinct packs of core-segments in orbit, as proposed in Eq.(3.1.1b). If so, then Eq.(4.1) would involve a mass defect, such that the binding energy of creation has reduced ($3 \times 69 m_e$) to:

$$m_\mu = 206.7682838 m_e \approx 3 \times 69 \left\{ 1 - \frac{\alpha}{2\pi} + \left(\frac{\alpha}{2\pi} \times \frac{\pi^2 \alpha}{2} \right) \right\} m_e \quad . \quad (4.2)$$

This expression relies on the electron mass being a fundamental unique quantity, but the free electron structure is much larger than the muon; so a muon is not a cluster of electrons.

Binding energy implies the existence of an attractive force which holds the muon together in spite of its many charged component parts, as discussed in Section 3. This is the guidewave force in operation, as seen in controlling the spiralling processes, and maintaining the charged helixes around the circumference of each species.

Therefore, the first quotient in Eq.(4.2) covers normalized spin-loop binding energy, calculated in the same way as electric self-interaction energy in Section 2:

$$\alpha / 2\pi = (e^2 / 2\pi r_\mu) / m_\mu c^2 . \quad (4.3)$$

The second term represents a kind of magnetic spin-orbit interaction energy, analogous to that in the hydrogen 1st Bohr orbit. In the muon spin-loop there are 137 orbiting charged core-segments which are confined by the guidewave force. These produce a magnetic field at the centre (MKS units):

$$B = \mu_o \frac{i}{2r_\mu} = \left(\frac{1}{\epsilon_o c^2} \right) \left(\frac{1}{2r_\mu} \right) \left(\frac{e}{2\pi r_\mu / c} \right) . \quad (4.4)$$

This reacts back on each core-segment to cause an energy shift because a core-segment has its own magnetic moment μ_{cs} due to its peripheral pearl charges:

$$\mu_{cs} = \text{current} \times \text{area} = \left[\frac{(e/137)c'}{2\pi r_o'} \right] \left[\pi r_o'^2 \right] . \quad (4.5)$$

Therefore the energy shift for all 137 core-segments is nominally:

$$\Delta E = 137 \mu_{cs} B . \quad (4.6)$$

However, the core-segments consist of a pearly helix which is continually changing direction. So an average energy shift will be:

$$\delta E = \left(\frac{2}{\pi} \right) \Delta E = \frac{e^2}{4\pi \epsilon_o (2\pi r_\mu)} \left(\frac{\pi^2 / 2}{137} \right)_{\text{cgs.units}} \rightarrow \frac{\alpha}{2\pi} \left(\frac{\pi^2 / 2}{137} \right) m_\mu c^2 . \quad (4.7)$$

After normalisation by $m_\mu c^2$, this is the required energy shift factor. Its effect is to reduce the main electric binding energy component.

The electron, muon, and tauon constitute a family of leptons, which have very different masses related by:

$$\begin{aligned} m_\mu &= 206.768 m_e \approx m_e (3 \times 69) , \\ m_\tau &= 3477.48 m_e \approx m_e (3 \times 69^{5/3}) . \end{aligned} \quad (4.8)$$

One explanation for this apparent connection, involving factor 69, can be based upon our pending proton and charmonium models, as follows. Quigg and Rosner's (1979) paper showed how charmonium could consist of a quark and anti-quark bound together by a gluonic force which obeys a logarithmic potential function like:

$$V(r) = \frac{m_c c^2}{2\sqrt{2}} \ln\left(\frac{r}{r_q}\right), \quad (4.9)$$

where m_c and r_q are the charmonium characteristic mass and separation of the quark and anti-quark. Similarly for the proton, this expression for gluonic binding energy becomes:

$$V(r) = \frac{m_p c^2}{3\sqrt{2}} \ln\left(\frac{r}{r_p}\right), \quad (4.10)$$

where m_p is the mass and ($r_p = 137e^2/m_p c^2$) is the spin radius. Factor 3 has been attributed to the 3 main components of the proton, which themselves consist of 3 parts.

Now for the muon, we shall employ a similar expression for the electromagnetic guidewave force which binds it together; but it is the 3 packs of core-segments (of mass $m_{\mu a} = m_{\mu}/3$) which are being described. Let the internal binding energy of a single muon pack be given by:

$$V(r) = \frac{m_{\mu a} c^2}{3\sqrt{2}} \ln\left(\frac{m_{\mu a}}{m_e}\right) = \frac{m_{\mu a} c^2}{3\sqrt{2}} \ln\left(\frac{r_{oe}}{3r_{\mu o}}\right), \quad (4.11)$$

where ($r_{oe} = e^2/m_e c^2$) and ($r_{\mu o} = e^2/m_{\mu} c^2$) are classical radii of the electron and muon. Then for the maximum binding energy ($V(r) = m_{\mu a} c^2$ say), we get ($\ln 69 \approx 3 \times 2^{1/2}$) which accounts for the factor 69.

By analogy, let the tauon's pack of core-segments have internal binding energy given by:

$$V(r) = \frac{m_{\tau a} c^2}{5\sqrt{2}} \ln\left(\frac{m_{\tau a}}{m_e}\right) = \frac{m_{\tau a} c^2}{5\sqrt{2}} \ln\left(\frac{r_{oe}}{3r_{\tau o}}\right), \quad (4.12)$$

where mass ($m_{\tau a} = m_{\tau}/3$). And for maximum binding energy ($V(r) = m_{\tau a} c^2$ say), we get ($\ln[3477/3] \sim 5 \times 2^{1/2} \approx (5/3)\ln 69$). Consequently, given that charmonium has 2 components and a proton has 3 components, and a muon pack has 3 sub-components, then the tauon pack probably has 5 sub-components.

Furthermore, by inference, if a more massive lepton can exist, (named a hepton from Greek 7), it could have a pack of 7 sub-components and overall mass around:

$$m_{\zeta} \approx m_e [3 \exp(7\sqrt{2})] \approx m_e (3 \times 69^{7/3}) \approx 58,500 m_e \approx 29.9 \text{ GeV} / c^2 \quad . \quad (4.13)$$

Production of this plus its anti-particle in an e^+e^- collision would require a 60 GeV centre-of-mass energy. However, the standard data analysis implies that there is no place for another lepton.

5. Muon lifetime

Muons are regarded as relatively stable particles because their path lengths exceed their Compton wavelengths by around 5×10^{16} times. Such a ratio by itself is incomprehensible, but it might be interpretable in terms of internal *action* within a muon. The lifetime is defined as the average time for an initial number of muons to decay exponentially by a factor e_n . Experimentally it has the value:

$$\tau_{\mu} = 2.197\,034 \times 10^{-6} \text{ secs} \quad . \quad (5.1)$$

From Section 3.2, the muon core-segment period may be evaluated accurately as:

$$t_{\mu 0} = 'O_0/c' = \alpha h / m_{\mu} c^2 = 2.856\,321 \times 10^{-25} \text{ secs} \quad , \quad (5.2)$$

where $h = 6.626\,06896(33) \times 10^{-34} \text{ Js}$, and $c = 299\,792\,458 \text{ ms}^{-1}$. Now Eq.(3.2.2), which expresses the action around a core-segment's helix of 37.7 spinning pearls, was based on the formula,

$$\ln 37.7 \approx 2(\pi/2)(\pi/e_n) \quad . \quad (5.3)$$

In an analogous way, let $(c' \tau_{\mu})$ equal a number N_{μ} of core-segment circumferences $'O_0$; then upon taking a logarithm we have:

$$\ln(c' \tau_{\mu} / 'O_0) = 43.486\,691 \approx 24(\pi/2)(\pi/e_n) \quad . \quad (5.4)$$

Muon pearls are spinning at velocity c' in Eq.(3.2.2), and they also propagate at velocity c' around the core-segment circumference. Then Eq.(5.4) may be developed in the usual way to give an action integral like Eq.(3.2.2) for the action over N_{μ} core-segments:

$$\int_{O_0}^{N_\mu O_0} \frac{(e/137)^2}{y} \frac{dy}{c'} \approx 24 \times \int_0^{2\pi} \frac{m_\mu c r_{\mu o}}{2 \times 137^2} \left(\frac{1}{e_n} \right) d\theta . \quad (5.5)$$

Clearly, a second harmonic guidewave is involved in this action, as it is in Eq.(3.2.2); so one possible explanation for τ_μ is that $(c' \tau_\mu)$ represents a *coherence length* which governs muon stability. The weighting coefficient 24 is unexplained but it is responsible for the very long muon lifetime, and makes this action equal to 12 times that in Eq.(3.2.2).

6. Some features of a tauon model

Tauon mass and lifetime have been measured accurately enough to justify postulating some design features. A preliminary attempt at explaining the muon mass m_μ and tauon mass m_τ was made in Section 4. Now, the measured tauon mass relative to electron mass is:

$$m_\tau/m_e = 3477.48(57) , \quad (6.1)$$

which may be expressed as:

$$m_\tau \approx 50 \times 69 m_e \approx (16\pi/3) m_\mu . \quad (6.2)$$

This is interesting because 69 and 16π are factors of the muon model.

Lifetime of the tauon is short compared with the muon, but long enough to be interpreted in a similar manner:

$$\tau_\tau = 290.6(1.0) \times 10^{-15} \text{ secs} . \quad (6.3)$$

Core-segment period in the tauon will be given by an expression like Eq.(5.2):

$$t_{\tau o} = \alpha h / m_\tau c^2 \approx 1.698 \ 29 \times 10^{-26} \text{ secs} . \quad (6.4)$$

Let $c'\tau_\tau$ equal a number N_τ of core-segment circumferences ($c't_{\tau o}$), then after taking a logarithm we have:

$$\ln \left(\frac{c'\tau_\tau}{c't_{\tau o}} \right) = 30.471 \approx \left(\frac{16\pi}{3} \right) \left(\frac{\pi}{2} \right) \left(\frac{\pi}{e_n} \right) . \quad (6.5)$$

This compares well with Eq.(5.4) and it may be developed to give an action integral equation, similar to Eq.(5.5):

$$N_{\tau} \int_{2\pi r'_{\tau o}}^{2\pi r'_{\tau o}} \frac{(e/137)^2}{y} \frac{dy}{c'} \approx \left(\frac{16\pi}{3}\right) \times \int_0^{2\pi} \frac{m_{\tau} c r_{\tau o}}{2 \times 137^2} \left(\frac{1}{e_n}\right) d\theta . \quad (6.6)$$

As for the muon, $(c'\tau_{\tau})$ could represent a *coherence length* which governs tauon stability.

7. Conclusion

A geometrical/mechanical model of the muon has been derived, which is similar in many respects to the previous electron model. There are again five levels of species from the spin-loop to fundamental elements. Calculation of the anomalous magnetic moment has been done in geometrical terms, and the lifetime interpreted as a coherence time. Mass and lifetime of the tauon have also been accommodated within the general scheme.

Acknowledgement

I would like to thank Imperial College Library staff and A. Rutledge for typing.

References

Quigg C and Rosner J L 1979 *Phys Reports* **56** 167-235

Wayte R Paper 1, A Model of the Electron, submitted to *Journal of Physics G*